

Ammonium Bisulfate/Water: A Pseudobinary System

Keith D. Beyer* and Jameson Bothe

Department of Chemistry, University of Wisconsin—La Crosse, La Crosse, Wisconsin 54601

Received: December 28, 2005; In Final Form: April 3, 2006

We have studied the ammonium bisulfate/water system using thermal analysis (differential scanning calorimetry) and infrared spectroscopy of thin films. Our results for the melting points for ice and letovicite are in good agreement with other experimental work. However, we report here the first measurements of the ice/ammonium bisulfate/letovicite invariant point. We have used our observations and solubility data to construct a complete phase diagram for this system. Utilizing phase diagram theory and the Gibbs phase rule, we conclude that this system is not a true binary system but rather a pseudobinary system, which has a range of concentrations that cannot be represented by a simple binary phase diagram and thus must be viewed as part of the ternary system: $\text{H}_2\text{SO}_4/(\text{NH}_4)_2\text{SO}_4/\text{H}_2\text{O}$. We also compared our results to the phase diagram predictions of the aerosol inorganics model and found the predicted melting points are in good agreement with experimental work over a limited concentration range, but the transitions predicted by the model at lower temperatures are not in agreement with experimental results.

Introduction

Tropospheric aerosols are made up predominantly of aqueous ammonium and sulfate ions with the molar ratio of $\text{NH}_4^+/\text{SO}_4^{2-}$ ranging from 0 to 2.^{1,2} Observations during the subsonic aircraft: contrail and cloud effects special study (SUCCESS) revealed free tropospheric aerosols containing significant amounts of NH_4^+ and SO_4^{2-} including conditions where cirrus ice was present.³ Also, theoretical studies have shown the importance of ammoniated sulfate aerosols in cirrus cloud formation.^{4,5} These particles absorb and scatter solar radiation dependent upon their phase, thus contributing to the radiation balance.⁶ They may also play a significant role in heterogeneous chemistry in the troposphere.⁷ In all of these cases, understanding the thermodynamic properties at low temperatures is critical to knowing which phases may be present when particles crystallize. Therefore, the thermodynamics of these systems needs to be studied to better understand tropospheric aerosols, aerosol chemistry, and cloud formation mechanisms.

The $\text{NH}_4\text{HSO}_4/\text{H}_2\text{O}$ system is a subsystem of the $\text{H}_2\text{SO}_4/(\text{NH}_4)_2\text{SO}_4/\text{H}_2\text{O}$ system, consisting of a constant 1:1 mole ratio of $\text{H}_2\text{SO}_4:(\text{NH}_4)_2\text{SO}_4$. The low-temperature phase diagram of $\text{H}_2\text{SO}_4/(\text{NH}_4)_2\text{SO}_4/\text{H}_2\text{O}$ has been little studied; it has been constructed from solubility data at 273 K and above.^{8–10} Research at lower temperatures has focused on the $\text{NH}_4\text{HSO}_4/\text{H}_2\text{O}$ subsystem. Studies have been performed to determine nucleation of solid phases in $\text{NH}_4\text{HSO}_4/\text{H}_2\text{O}$ samples using various techniques: single particle levitation,^{11,12} emulsions and optical microscopy of small droplets and thermal analysis of bulk solutions,¹³ vapor pressures of bulk solutions,^{14,15} and particle flow tube techniques.^{16,17} Many of these studies have detected the formation of ice, and some have determined the formation of letovicite, $(\text{NH}_4)_3\text{H}(\text{SO}_4)_2$ (3:1 mole ratio of $(\text{NH}_4)_2\text{SO}_4:\text{H}_2\text{SO}_4$), and still others have detected hydrate formation¹² (though these results have not yet been confirmed by other investigators). As a result of these studies, melting points of ice, the temperature dependence of letovicite deliquescence, the

ice/letovicite “eutectic” at 243 K, and the temperature of a ternary eutectic at 196 K (assigned to ice/SAT/letovicite by Koop et al.¹³) have been reported for the $\text{NH}_4\text{HSO}_4/\text{H}_2\text{O}$ system. However, each of these studies has interpreted their results in a slightly different way leading to different pictures of the $\text{NH}_4\text{HSO}_4/\text{H}_2\text{O}$ phase diagram.

Experimental Section

Sample Preparation. Ammonium bisulfate samples were prepared by diluting 98 wt % ACS reagent grade H_2SO_4 and 99.99 wt % ACS reagent grade $(\text{NH}_4)_2\text{SO}_4$ supplied by Fisher or Aldrich in a constant 1:1 mole ratio with Culligan purified water. Concentrated sulfuric acid was standardized by acid–base titration. The concentration of all samples is known to ± 0.00063 mol fraction.

Infrared Spectra. The sample cell used for infrared spectra is shown schematically and explained in detail in previous literature¹⁸ and our detailed method is given in Hansen and Beyer.¹⁹ Sample volumes were 1–2 μL . The IR cell temperatures are known on average to within ± 1.3 K; i.e., a temperature we measured in the IR cell of a specific transition is within 1.3 K of the transition temperature we measure (of the same transition) using the DSC. Spectra were obtained with a Bruker Tensor 37 FTIR with an MCT-B detector at 16 cm^{-1} resolution. Each spectrum is the average of four scans. Samples were cooled to 192 K at 3 K min^{-1} and then allowed to warm to room temperature without resistive heating, typically this was 1 K min^{-1} .

Differential Scanning Calorimeter. Thermal data were obtained with a Mettler Toledo DSC 822e with liquid nitrogen cooling, and industrial grade nitrogen gas was used as a purge with a flow rate of 50 mL min^{-1} . The temperature reproducibility of this instrument is better than ± 0.05 K. Our accuracy is estimated to be ± 0.9 K with a probability of 0.94 on the basis of a four-point temperature calibration.²⁰ Samples were contained in a 30, 70 or 150 μL platinum pan, depending on sample size. Sample masses ranged between 20 and 90 mg. A typical sample was cooled to 183 K at 10 K min^{-1} , held at that

* Corresponding author. E-mail: Beyer.Keith@UWLAX.EDU.

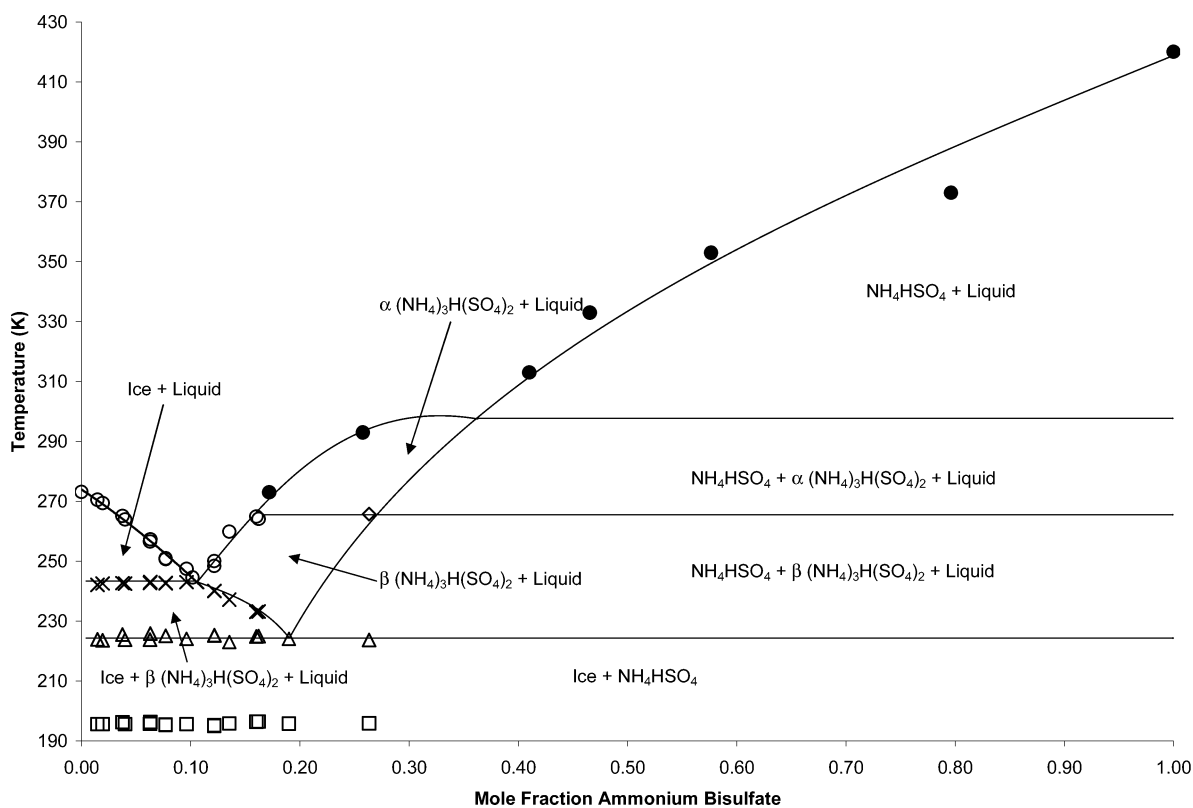


Figure 1. $\text{NH}_4\text{HSO}_4/\text{H}_2\text{O}$ pseudobinary phase diagram. Data from this study: (○) melting points; (×) ice/letovicite phase boundary; (△) liquid + ice + letovicite + ammonium bisulfate invariant point; (□) SAT decomposition; (◇) letovicite solid/solid-phase transition. (●) Literature solubility points from Linke.⁸

temperature for 5 min, and then warmed at a rate of 1 K min^{-1} until a point at least 5 K above the final melting point.

Results

Figure 1 shows the phase diagram of ammonium bisulfate/water as a function of temperature and mole fraction of NH_4HSO_4 constructed from our DSC and IR results along with literature solubility data for the respective solids of this system for temperatures above 273 K.⁸ All samples corresponding to solutions in the ice and letovicite primary phase fields, respectively, displayed identical transitions (except the freezing point depression, which changed with concentration). Therefore, we will discuss the thermogram and IR spectra of a single sample on each side of the ice/letovicite phase boundary in detail as being typical of all samples in these phase regions.

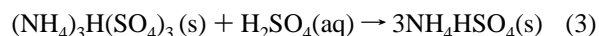
A sample with concentration of 0.063 mol fraction NH_4HSO_4 lies under the ice primary phase field as seen in Figure 1. A cooling/warming thermogram of this sample is given in Figure 2, and the IR spectra as a function of temperature for cooling are given in Figure 3 and warming in Figure 4. In the IR experiment (Figure 3) ice forms at 232 K during the cooling segment. In the DSC experiment (Figure 2) this crystallization occurs at 241 K, most likely because of the much larger sample size. Letovicite forms at 211 K in the IR experiment as evidenced by the shift in the NH_4^+ peak from $1456 \rightarrow 1424 \text{ cm}^{-1}$, the diminishment of the HSO_4^- peaks at 1051 and 884 cm^{-1} , and the growth of the SO_4^{2-} peak at 1114 cm^{-1} , which is characteristic of letovicite.²¹ In the DSC experiment this transition occurs at 221 K, again slightly higher than that in the IR experiment. This mixture of ice/letovicite/liquid persists until 176 K when SAT appears to form given by the appearance of the SO_4^- peak at 1074 cm^{-1} , and a small increase in the HSO_4^- peak at 884 cm^{-1} (see Beyer et al.²² for reference

spectra). In the DSC this transition occurs during the isothermal segment at 184 K.

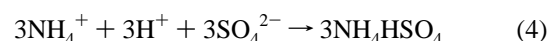
In the warming segment the DSC and IR melting transition temperatures correspond exactly because these processes are always occurring under equilibrium conditions. Upon warming from 176 K, the IR spectra are constant until 196 K when SAT melts (Figure 4), which is seen as an endothermic transition in the thermogram of Figure 2:



The thermogram indicates a recrystallization of the melt begins just after the melting transition completes. In the IR experiment we observe a slow formation of NH_4HSO_4 at the expense of letovicite over the temperature range 207–218 K, as indicated by the growth of the HSO_4^- peak at 1040 cm^{-1} and the diminishing of the SO_4^{2-} peak at 1115 cm^{-1} .²³ Although it is difficult to quantify the crystallization of ice as the water from SAT freezes using the IR data, it is reasonable to assume ice forms along with the reaction of the aqueous ammonium, protons, and sulfate into ammonium bisulfate. Therefore, the exothermic “recrystallization” is represented by the following two reactions:



Equation three may be rewritten in an ionic form as



After the recrystallization, the spectra remain constant, indicating a mixture of ice and NH_4HSO_4 until 224 K when a rapid

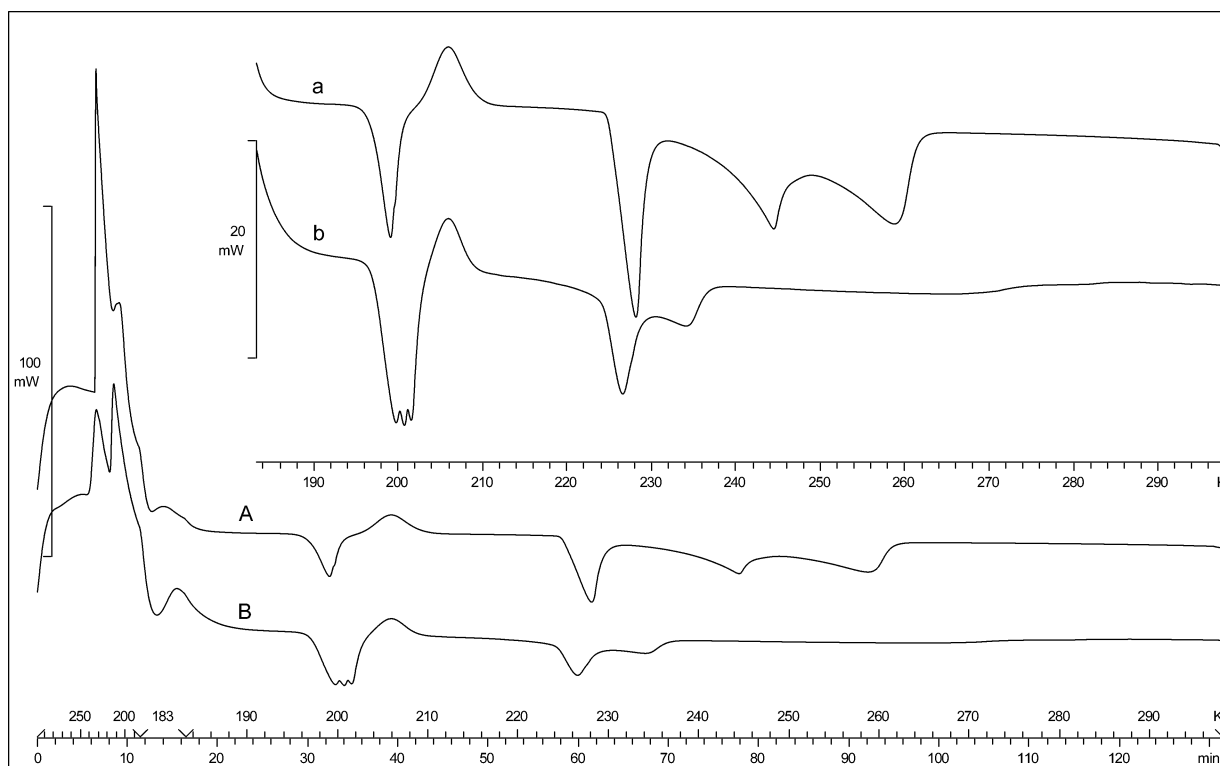


Figure 2. DSC thermograms (exotherms point up) of ammonium bisulfate solutions. Capital letters are cooling and warming segments; small letters are expansions of the warming segment (mole fraction): A/a, 0.063; B/b, 0.162. The 0.063 mole fraction sample corresponds to a concentration under the ice primary phase field, and the 0.162 mole fraction sample is in the letovicite primary phase field.

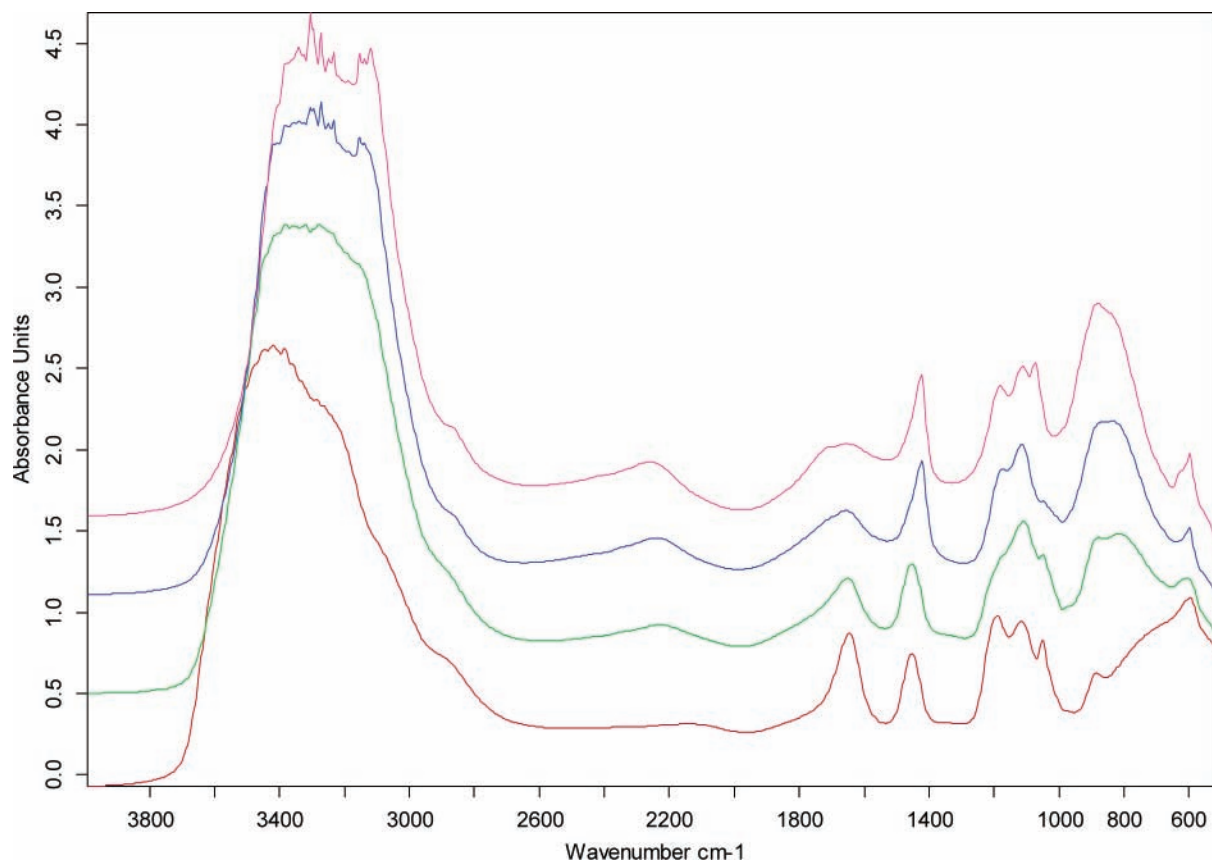


Figure 3. Infrared spectra for cooling of a 0.063 mol fraction NH_4HSO_4 sample: red, completely liquid sample at 291 K; green, 232 K showing ice formation; blue, 211 K showing letovicite formation; purple, 176 K showing SAT formation. Spectra are offset by the following (absorbance units): red, 0.0; green, +0.5; blue, +1.0; purple, +1.5.

conversion from $\text{NH}_4\text{HSO}_4 \rightarrow (\text{NH}_4)_3\text{H}(\text{SO}_4)_2 + \text{liquid}$ occurs, completing at 226 K. In the IR spectra, we observe the rapid

reversal of the peak shifts that occurred in the conversion of letovicite to NH_4HSO_4 . This transition appears as an endotherm

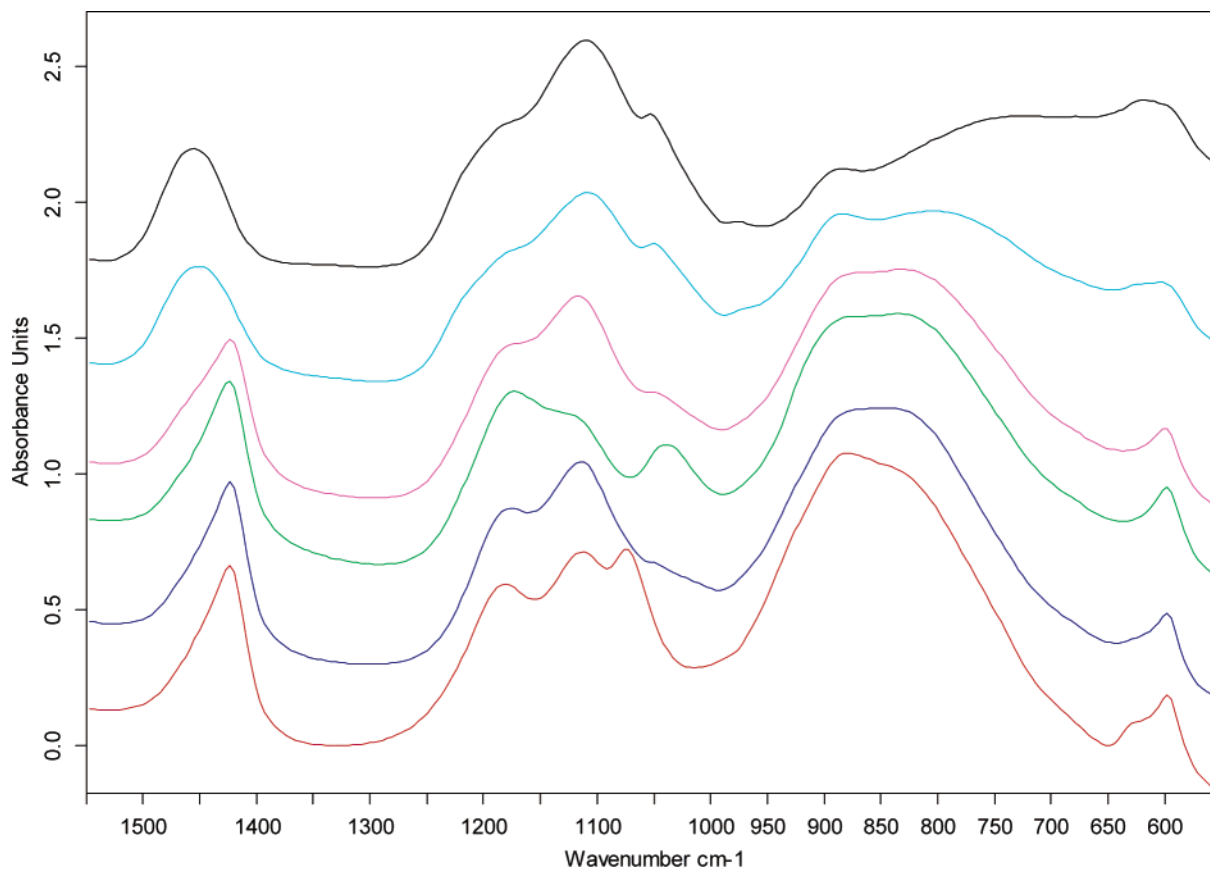


Figure 4. Infrared spectra for warming of a 0.063 mol fraction NH_4HSO_4 sample: red, 195 K just before SAT melt; blue, 197 K SAT melted leaving signatures of ice and letovicite; green, 218 K at the completion of the conversion of letovicite $\rightarrow \text{NH}_4\text{HSO}_4$; purple, 226 K at the completion of the conversion of $\text{NH}_4\text{HSO}_4 \rightarrow$ letovicite; light blue, 242 K completion of letovicite melt; black, 257 K completion of ice melting. Spectra are offset by the following: red, -0.3 ; blue 0.0 ; green, $+0.4$; purple, $+0.6$; light blue, $+1.0$; black, $+1.4$.

in the DSC thermogram in Figure 2. The observation that liquid remains after this transition is clearly seen in the thermogram (as the sample is heated to higher temperatures) by the significant slope of the baseline, which indicates liquid in contact with a solid undergoing a transition. The reverse of eq 3 makes it clear that liquid H_2SO_4 must be present. This liquid will likely melt some of the ice, forming an aqueous solution. From 226 to 243 K the letovicite is slowly melting (dissolving). This phase transition is seen in the thermogram, and in the IR spectra as the NH_4^+ peak begins to shift back from $1425 \rightarrow 1454 \text{ cm}^{-1}$ and the HSO_4^- peaks at 1051 and 884 cm^{-1} begin to reappear as these ions form in solution. Finally, ice melts over the range $243\text{--}257 \text{ K}$, as indicated by the endotherm in the thermogram (Figure 2) and by shifts in the IR spectra.

The phase transition pattern for a sample in the letovicite primary phase field (0.162 mole fraction NH_4HSO_4) is similar to that for the sample in the ice primary phase field. In the thermogram (Figure 2) three crystallization events are seen at 244, 222, and 184 K. The IR spectra display the same shifts as for the 0.063 mole fraction sample; however, they appear in a different order. Letovicite forms at 223 K, whereas ice forms at 209 K. At 171 K SAT forms. Thus, as expected, the order of crystal formation for a sample in the letovicite primary phase field is: letovicite, ice, SAT. Upon warming, SAT melts at 195 K (IR experiment); however, the thermogram displays three closely spaced endothermic transitions over the temperature range of $196\text{--}200 \text{ K}$ (see Figure 2). From the IR experiment, it is clear one of these transitions is the melting of sulfuric acid tetrahydrate (SAT). We suspect one of the two remaining transitions is the melting of sulfuric acid octahydrate (SAO);

we are unable to identify the third transition. Because the fraction of the sample in the latter two phases is likely small, we do not have specific IR evidence for their presence. In the temperature range $210\text{--}218 \text{ K}$ the conversion from letovicite $\rightarrow \text{NH}_4\text{HSO}_4$ occurs, as evidenced in the IR experiment by the peak shifts given above. In the DSC experiment, this transition occurs immediately after the completion of the SAT melt and likely corresponds to the exotherm at $203\text{--}209 \text{ K}$. Then at $223\text{--}224 \text{ K}$ the reverse reaction occurs (same in IR and DSC experiments). Following that, ice melts continuously from $226 \rightarrow 233 \text{ K}$, followed by the continuous melting of letovicite to its solubility point at 264 K (see Figure 2).

Analysis

It is immediately apparent that this system does not represent a typical binary phase diagram. First, the ice/letovicite phase boundary at $242.6 \pm 0.3 \text{ K}$ appears on the water-rich side of the phase boundary, but on the letovicite-rich side the temperature of this transition becomes a function of sample concentration. Second, we have measured an invariant point at approximately 0.19 mole fraction NH_4HSO_4 (which has not been previously reported) where liquid, ice, letovicite, and ammonium bisulfate all coexist at $223.6 \pm 0.2 \text{ K}$. The Gibbs phase rule is

$$F = C - P + 1 \quad (\text{pressure is fixed}) \quad (5)$$

where F is the number of degrees of freedom, C is the number of components, and P is the number of phases. At this invariant point the number of degrees of freedom is -1 , making this point physically unreal in a binary system. Finally, the $\text{NH}_4\text{HSO}_4/$

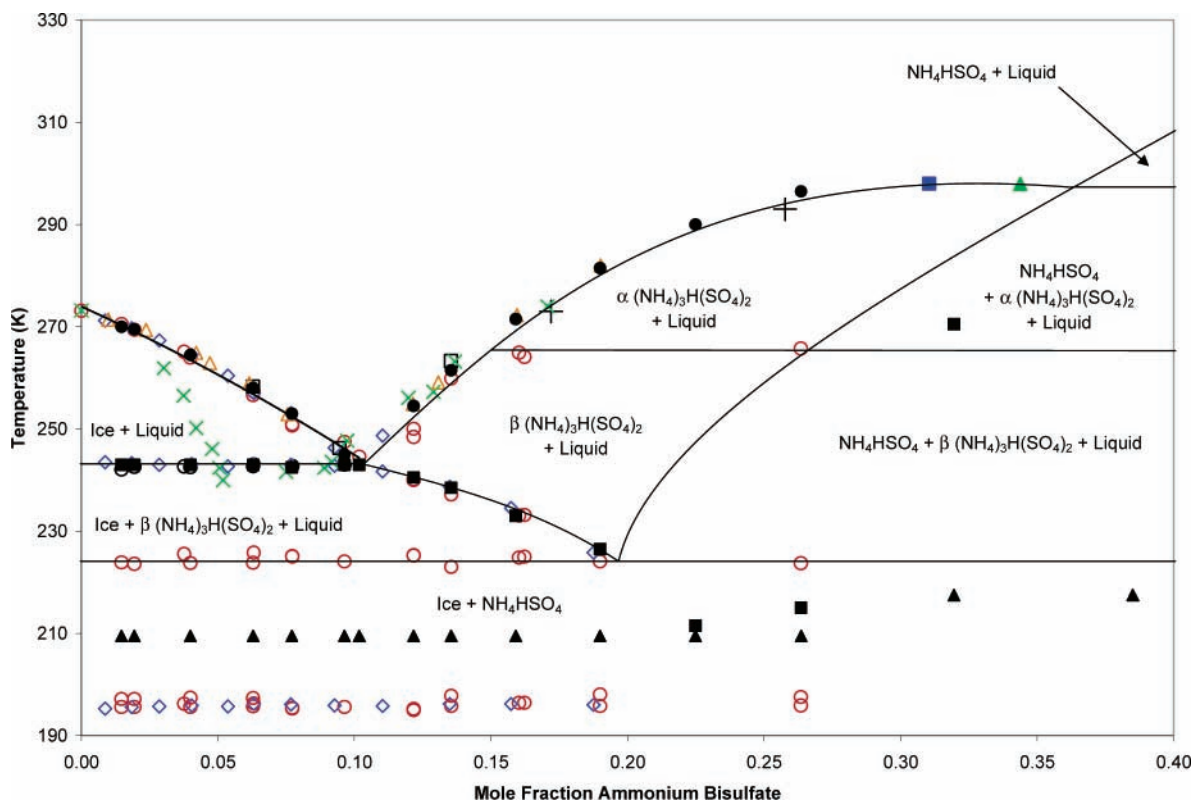


Figure 5. Expansion of the $\text{NH}_4\text{HSO}_4/\text{H}_2\text{O}$ pseudobinary phase diagram showing data from this study (red open circles) and that from the literature: blue diamonds, Koop et al.;¹³ orange triangles, Chelf and Martin;¹⁵ green exes, Imre et al.;¹² black open squares, Yao et al.;¹⁶ black crosses, Linke;⁸ solid blue square, Tang and Munkelwitz;¹⁶ solid green triangle, Spann and Richardson.¹¹ AIM predictions:²⁵ solid black circles, final melting point; solid black squares, ice/letovicite phase boundary; solid black triangles, ice/SAH/letovicite ternary eutectic.

H_2O system produces a stable molecular solid, $(\text{NH}_4)_3\text{H}(\text{SO}_4)_2$ at moderate concentrations of NH_4HSO_4 upon cooling. However, this solid cannot be produced from any combination of H_2O and NH_4HSO_4 . These observations necessitate the conclusion that the $\text{NH}_4\text{HSO}_4/\text{H}_2\text{O}$ system is not a true binary system, but rather a slice of constant 1:1 ratio of $(\text{NH}_4)_2\text{SO}_4:\text{H}_2\text{SO}_4$ in the $\text{H}_2\text{SO}_4/(\text{NH}_4)_2\text{SO}_4/\text{H}_2\text{O}$ ternary system. However, ice and ammonium bisulfate do share a phase boundary; therefore, the $\text{NH}_4\text{HSO}_4/\text{H}_2\text{O}$ system can be viewed as a pseudobinary system or a “join”.²⁴ The result is that the concentration of the liquid below the letovicite melting envelope cannot be defined using the binary diagram of Figure 1. The total concentration of a sample after letovicite forms in the region below the melting envelope will not follow a straight vertical line but rather will curve as the liquid becomes more acidic than would be predicted by the diagram as first recognized by Chelf and Martin¹⁵ and Yao et al.¹⁴ However, the pseudobinary diagram is useful for comparing melting point data from several experiments reported in the literature as well as the predictions of the Aerosol Inorganics Model (AIM).²⁵

Figure 5 is an expansion of the phase diagram of Figure 1. On this figure we have plotted our data as well as data from the literature and the predictions of the AIM. There is very good agreement between all experimental data except that of Imre et al.¹² Along with other investigators, we did not see evidence for an ammonium bisulfate octahydrate reported by Imre et al. However, we did observe low-temperature transitions (195.6 ± 0.3 K) that Koop et al.¹³ assigned to an ice/SAT/letovicite ternary eutectic on the basis of the predictions of AIM. However, the AIM only predicts this transition when the formation of sulfuric acid hemihydrate (SAH) is suppressed. In our experiments, the IR results show clear signatures of SAT along with ice and letovicite at temperatures below 195 K. We observe

the loss of SAT at 195 K, similar to the case for the endotherm observed by Koop et al.; however, we also observed a rapid recrystallization of the SAT melt, which was not seen by Koop et al. Interestingly, when SAH is not suppressed in the AIM, it predicts an ice/SAH/letovicite eutectic at 209.5 K for concentrations below 0.26 mole fraction NH_4HSO_4 . At higher concentrations, the AIM predicts this eutectic at 217.5 K. These results are plotted in Figure 5. There has been no reported experimental evidence for such a transition in the literature.

To determine if our observations could be interpreted as a combination of ice/SAH/letovicite below 224 K, we have compared our IR spectra with the spectral addition of ice/SAH/letovicite and the spectral addition of ice plus ammonium bisulfate crystals (Figure 6). The ice spectrum was obtained in the same manner as given in the Experimental Section. The ammonium bisulfate spectrum was obtained by dissolving NH_4HSO_4 crystals (>99.5% Fluka) in anhydrous ethanol to saturation. Several drops of the solution were placed successively on the ZnSe window and allowed to dry in intervals to build up a film of sufficient thickness for a transmission spectrum. The letovicite spectrum was obtained from a completely frozen sample of ice/letovicite with the ice features subtracted to bring the OH peak at ~ 3300 cm^{-1} to baseline. The resulting spectrum is in excellent agreement with that given by Damak et al.²¹ for letovicite. The SAH spectrum was prepared as given in Beyer et al.²² To account for differences in film thicknesses (hence differences in absorbance), the individual spectra were reduced or increased before addition: the OH peak at ~ 3300 cm^{-1} for SAH and ice was equalized, the broad $\text{SO}_4^{2-}/\text{HSO}_4^-$ peaks at 1130/1190 cm^{-1} were equalized for the ice + SAH and letovicite addition. For ice + NH_4HSO_4 , the baselines were equalized in the range 2700–1900 cm^{-1} . Upon comparison of the spectra, one peak appears

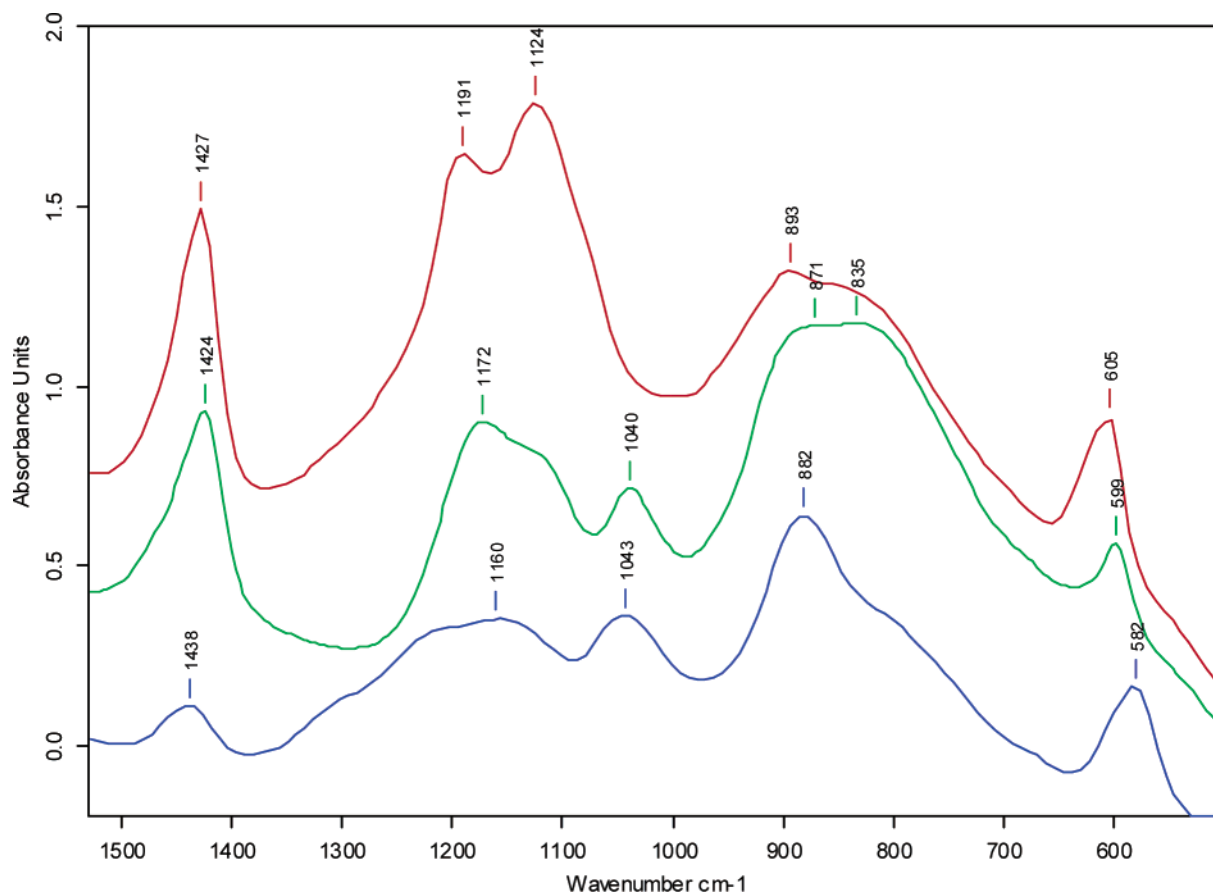


Figure 6. Green spectrum: same as that in Figure 4. Red spectrum: spectral addition of ice + letovicite + sulfuric acid hemihexahydrate spectra. Blue spectrum: spectral addition of ice + ammonium bisulfate film, offset by -0.6 absorbance units for clarity.

to be characteristic of NH_4HSO_4 , the HSO_4^- peak at $\sim 1040\text{ cm}^{-1}$. This peak appears as a broad peak centered at 1035 cm^{-1} in the work of Miller and Wilkins²³ who acquired IR spectra of samples in Nujol mulls. This peak also appears in our spectral addition of ice + NH_4HSO_4 centered at 1043 cm^{-1} . The peak is completely absent in the spectral addition of ice/SAH/letovicite. Another piece of evidence that our samples do not contain SAH is the fact that the ice/SAH eutectic melt occurs at 211 K .²² Adding letovicite to create a ternary mixture would only depress the eutectic point, not increase it.

The peak at $\sim 580\text{--}600\text{ cm}^{-1}$ has been assigned to SO_4^- by Krost and McClenny,²⁶ whereas Schlenker et al.²⁷ assigned it to HSO_4^- (at 590 cm^{-1}) with an additional peak at 596 cm^{-1} assigned to HSO_4^- in letovicite. In work on dry ammonium bisulfate aerosols by Cziczko and Abbatt¹⁷ the peak is bifurcated. In our thin film spectra used to create the ice + ammonium bisulfate spectra in Figure 6, it appears as a single peak centered at 582 cm^{-1} ; however, in spectra obtained using an ATR accessory with ground NH_4HSO_4 crystals, the peak splits into three with centers at 605 , 583 and 570 cm^{-1} . Clearly the exact location of this peak is dependent on the crystal matrix and how it is prepared and would be difficult to use as the sole indicator for NH_4HSO_4 vs letovicite presence. Additionally, there appears to be a side shoulder peak at $\sim 1300\text{ cm}^{-1}$ in our ice + NH_4HSO_4 spectra (Figure 6). This side shoulder is apparent in the NH_4HSO_4 spectra from our thin film and ATR experiments, as well as that of others.^{17,26,27} However, the side shoulder does not clearly appear in our water/ NH_4HSO_4 spectra (green spectra in Figures 4 and 6). We do not have an explanation for why this might be the case other

than differences in crystal matrixes between our ice/ NH_4HSO_4 experiments and those where only pure NH_4HSO_4 crystals are present.

We observed a transition at $223.8 \pm 0.4\text{ K}$ in both our DSC and IR experiments that we have assigned to the invariant point conversion of $\text{NH}_4\text{HSO}_4 \rightarrow (\text{NH}_4)_3\text{H}(\text{SO}_4)_2$. This transition was not observed in the DSC experiments of Koop et al., nor is it predicted by the AIM. As mentioned above, we observed the recrystallization of the SAT melt in our experiments whereas Koop et al. did not. Our IR experiments show that this exotherm corresponds to the conversion of $(\text{NH}_4)_3\text{H}(\text{SO}_4)_2 \rightarrow \text{NH}_4\text{HSO}_4$. Because this transition did not occur in the Koop et al. experiments, it is a logical conclusion that they would not observe the conversion of $\text{NH}_4\text{HSO}_4 \rightarrow (\text{NH}_4)_3\text{H}(\text{SO}_4)_2$ at 223.8 K as seen in our experiments. Indeed, the significant slope to the baseline of the warming thermogram in their Figure 1 indicates the presence of liquid at temperatures above the SAT melt. To perform a direct comparison, we repeated the experiments of Koop et al. for several concentrations of NH_4HSO_4 and with varying sample mass. Four experiments are shown in Figure 7. The main differences between our experiments and those of Koop et al. are heating rate (1 vs 5 K/min) and sample size ($20\text{--}70$ vs $3\text{ }\mu\text{L}$). As seen in Figure 7, sample volume has no effect on the recrystallization of the SAT melt and appearance of the invariant point at 223.8 K . However, heating rate does. It is seen at the higher heating rate of 5 K/min , the SAT melt does not recrystallize independent of sample size. However, close inspection of the 5 K/min thermograms reveals a very small endotherm at 224 K . We interpret this as the invariant point conversion of $\text{NH}_4\text{HSO}_4 \rightarrow (\text{NH}_4)_3\text{H}(\text{SO}_4)_2$, as seen in

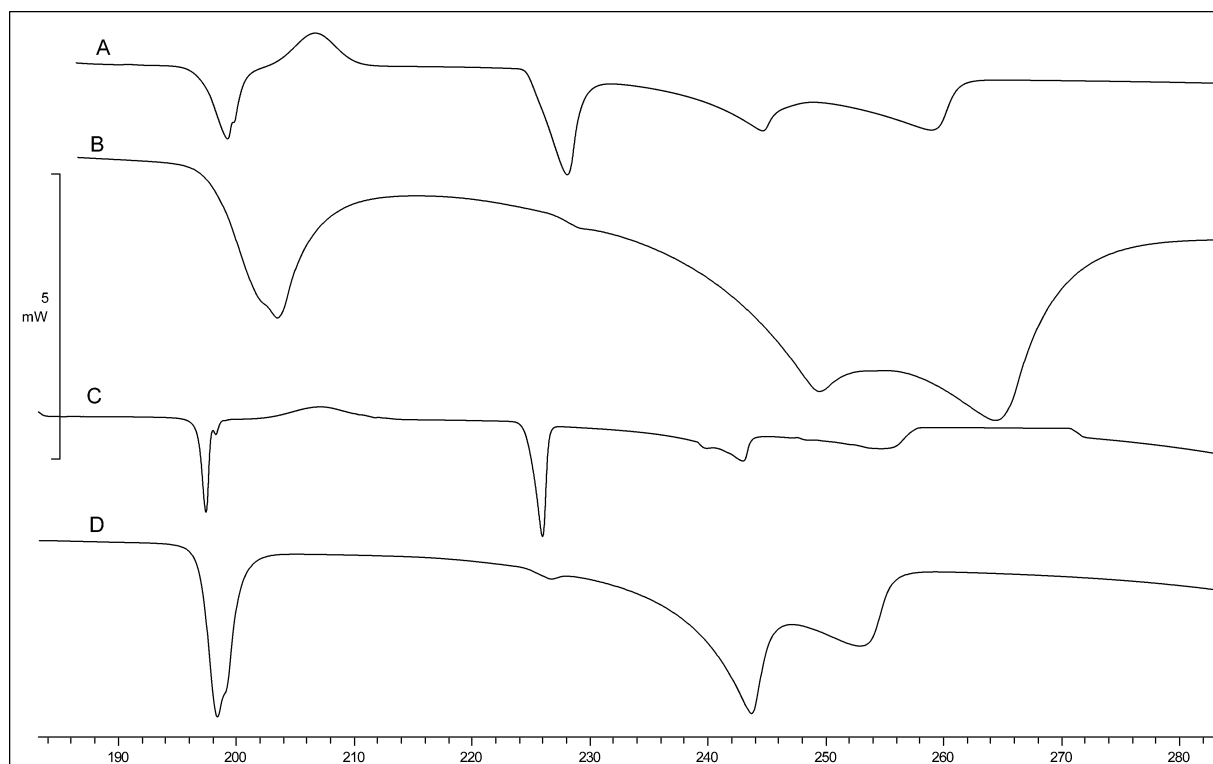


Figure 7. Thermograms of a 0.063 mole fraction sample of $\text{NH}_4\text{HSO}_4/\text{H}_2\text{O}$ at differing sample sizes and heating rates: A, 81.38 mg ($\sim 70 \mu\text{L}$) sample, 1 K/min heating rate; B, 82.28 mg ($\sim 70 \mu\text{L}$), 5 K/min heating rate; C, 3.33 mg ($\sim 3 \mu\text{L}$) 1 K/min heating rate; D, 3.27 mg ($\sim 3 \mu\text{L}$) 5 K/min heating rate. Thermograms A and B have been divided by 10 for presentation.

the 1 K/min experiments; however, the NH_4HSO_4 in this case must be a small amount that nucleated on cooling, but that was hindered from growth. Therefore, no recrystallization of the SAT melt occurred via nucleation on the small amount of ammonium bisulfate that was present. Hence, we conclude the heating rate is important in this system for the growth of ammonium bisulfate crystals. It is also interesting that at these high heating rates, we do not even have evidence for water crystallizing into ice from the SAT melt.

The higher temperature endothermic transitions of our experiments are in excellent agreement with the AIM and all other researchers except Imre et al.¹² (see Figure 5). On the basis of the results given here and the results of all other experimental observations (with exception of Imre et al. over a limited concentration range), we conclude there must be a fundamental error in the AIM predictions below 224 K for this system.

Conclusions and Atmospheric Implications

We have investigated the $\text{NH}_4\text{HSO}_4/\text{H}_2\text{O}$ system and, coupled with solubility data, have constructed a complete phase diagram for this system. Our data are in excellent agreement with other recent experimental work, except that of Imre et al.,¹² who concluded NH_4HSO_4 formed an octahydrate. We have no evidence for this solid. We report for the first time observation of the ternary invariant point for liquid/ice/ $\text{NH}_4\text{HSO}_4/(\text{NH}_4)_3\text{H}(\text{SO}_4)_2$ coexistence. On the basis of our results, we conclude that this system is a pseudobinary system, such that a significant portion of the phase diagram cannot be represented by a binary diagram. Agreement with the predictions of the aerosol inorganics model is good above 224 K. However, below this temperature the AIM predicts an ice/ $\text{SAH}/(\text{NH}_4)_3\text{H}(\text{SO}_4)_2$ invariant point at 209.5 K. Such a point has not been observed experimentally either in our work or that of others reported in the literature for this system. On the basis of our thermal analysis

and IR experiments, we conclude this invariant point does not exist in the $\text{NH}_4\text{HSO}_4/\text{H}_2\text{O}$ system. AIM predicts an ice/SAT/ $(\text{NH}_4)_3\text{H}(\text{SO}_4)_2$ eutectic at 197 K only when SAH formation is suppressed. This transition has been seen by Koop et al.¹³ and in our experiments.

Our results represent a shift in understanding this system at the low temperatures of the upper troposphere/lower stratosphere. The predictions of AIM indicate that ice does not coexist with NH_4HSO_4 , but our results indicate that it does. The AIM predicts that when an $\text{NH}_4\text{HSO}_4/\text{H}_2\text{O}$ aerosol completely crystallizes at concentrations less than 0.40 mole fraction (we did not investigate higher concentrations) solid ammonium bisulfate will not form. However, our results indicate that even if it does not form initially, NH_4HSO_4 is the thermodynamically stable phase in coexistence with ice and much or most of the letovicite present will convert to NH_4HSO_4 at temperatures below 223.8 K; however, we have evidence that growth of NH_4HSO_4 nuclei may be hindered at the low temperatures of the UT/LS. Our results indicate that ice and letovicite are likely to be the initial phases that form upon crystallization. SAT may form if temperatures are low enough for a long enough period of time. However, these solids will give way to the formation of ice and NH_4HSO_4 in the temperature range 195–223 K given enough time for NH_4HSO_4 nuclei to grow. A second significant result is the temperature above which liquid will exist in $\text{NH}_4\text{HSO}_4/\text{H}_2\text{O}$ aerosols. The AIM predicts liquid existence above 209.5 K. However, our results indicate little if any liquid will exist below 223.8 K. Because the interconversion of $(\text{NH}_4)_3\text{H}(\text{SO}_4)_2 \rightleftharpoons \text{NH}_4\text{HSO}_4$ is not stoichiometric, some liquid is likely to exist on one or the other side of this equation, especially under nonequilibrium conditions. However, it would be impossible to know a priori which side remaining liquid will exist on. Our experimental results indicate liquid existence

mainly above 223.8 K after the conversion $\text{NH}_4\text{HSO}_4 \rightarrow (\text{NH}_4)_3\text{H}(\text{SO}_4)_2$.

Acknowledgment. This work was supported by the National Science Foundation Atmospheric Chemistry Program (ATM-0304966 and ATM-0442273). We gratefully acknowledge the assistance of Niccola Burrmann who performed some of the DSC experiments.

References and Notes

- (1) Mason, B. J. *The Physics of Clouds*; Oxford University Press: New York, 1957.
- (2) Warneck, P. *Chemistry of the Natural Atmosphere*, 2nd ed.; Academic Press: San Diego, 2000; pp 405–428.
- (3) Talbot, R. W.; Dibb, J. E.; Loomis, M. B. *Geophys. Res. Lett.* **1998**, *25*, 1367–1370.
- (4) Tabazadeh, A.; Toon, O. B. *Geophys. Res. Lett.* **1998**, *25*, 1379–1382.
- (5) Martin, S. T. *Geophys. Res. Lett.* **1998**, *25*, 1657–1660.
- (6) Seinfeld, J. H.; Pandis, S. N. *Atmospheric Chemistry and Physics*; Wiley: New York, 1998; pp 440–446.
- (7) Hu, J. H.; Abbatt, J. P. D. *J. Phys. Chem. A* **1997**, *101*, 871–878.
- (8) Linke, A. *Solubilities of Inorganic and Metal Organic Compounds*, 4th ed.; American Chemical Society: Washington, DC, 1958.
- (9) Tang, I. N. *J. Aerosol Sci.* **1976**, *7*, 361–371.
- (10) Brosset, C. In *Atmospheric Sulfur Deposition*; Schriner, D. S., Ed.; Ann Arbor Science: Ann Arbor, MI, 1980; p 145–152.
- (11) Spann, J. F.; Richardson, C. B. *Atmos. Environ.* **1985**, *19*, 819–825.
- (12) Imre, D. G.; Xu, J.; Tang, I. N.; McGraw, R. *J. Phys. Chem. A* **1997**, *101*, 4191–4195.
- (13) Koop, T.; Bertram, A. K.; Molina, L. T.; Molina, M. J. *J. Phys. Chem. A* **1999**, *103*, 9042–9048.
- (14) Yao, Y.; Massucci, M.; Clegg, S. L.; Brimblecombe, P. *J. Phys. Chem. A* **1999**, *103*, 3678–3686.
- (15) Chelf, J. H.; Martin, S. T. *Geophys. Res. Lett.* **1999**, *26*, 2391–2394.
- (16) Tang, I. N.; Munkelwitz, H. R. *J. Aerosol Sci.* **1977**, *8*, 321–330.
- (17) Cziczo, D. J.; Abbatt, J. P. D. *J. Phys. Chem. A* **2000**, *104*, 2038–2047.
- (18) Zhang, R.; Wooldridge, P. J.; Abbatt, J. P. D.; Molina, M. J. *J. Phys. Chem.* **1993**, *97*, 7351–7358.
- (19) Hansen, A. R.; Beyer, K. D. *J. Phys. Chem. A* **2004**, *108*, 3457–3466.
- (20) Schubnell, M. J. *Thermal Anal. Calorim.* **2000**, *61*, 91.
- (21) Damak, M.; Kamoun, M.; Daoud, A.; Romain, F.; Lautie, A.; Novak, A. *J. Mol. Struct.* **1985**, *130*, 245–254.
- (22) Beyer, K. D.; Hansen, A. R.; Poston, M. *J. Phys. Chem. A* **2003**, *107*, 2025–2032.
- (23) Miller, F. A.; Wilkins, C. H. *Anal. Chem.* **1952**, *24*, 1253–1294.
- (24) Ehlers, E. G. *The Interpretation of Geological Phase Diagrams*; Dover: New York, 1987; pp 100–105.
- (25) Clegg, S. L.; Brimblecombe, P.; Wexler, A. S. *J. Phys. Chem.* **1998**, *102*, 2137–2154.
- (26) Krost, K. J.; McClenny, W. A. *Appl. Spectrosc.* **1994**, *48*, 702–705.
- (27) Schlenker, J. C.; Malinowski, A.; Martin, S. T.; Hung, H.; Rudich, Y. *J. Phys. Chem. A* **2004**, *108*, 9375–9383.